Peer-reviewed version available at Quantum Beam Sci. 2018, 2, 26; doi:10.3390/qubs2040026

Article

Influence of Concentration Fluctuations on Relaxation Processes in Spin Glasses

J. N. Wagner [1,2,3,4], W. Häußler [1,2], O. Holderer [5], A. Bauer [1], S. M. Shapiro [6] and P. Böni [1*]

1 Physik-Department E21, Technische Universität München, 85747 Garching, Germany
2 Heinz-Maier-Leibnitz-Zentrum (MLZ), Technische Universität München, Lichtenbergstr. 1, 85748 Garching, Germany
3 University of Stuttgart, Institute for Materials Science, Heisenbergstr. 3, 70569 Stuttgart, Germany
4 Karlsruhe Institute for Technology, KNMF and IAM-WK, Hermann-von-Helmholtz-Platz 1, 76344 Eggenstein-Leopoldshafen, Germany
5 Forschungszentrum Jülich GmbH, JCNS Outstation at MLZ, Lichtenbergstr.1, 85747 Garching, Germany
6 Brookhaven National Laboratory, Department of Physics, Upton, NY 11973, USA
* Correspondence: peter.boeni@frm2.tum.de; Tel.: +49-89-289-14711

Abstract: Using the unique combination of atomically resolved atom probe tomography (APT) and volume averaged neutron (resonance) spin echo (NRSE and NSE) experiments, the influence of nano-scaled clusters on the spin relaxation in spin glasses was studied. For this purpose, the phase transition from the paramagnetic phase to the spin glass phase in a Fe-Cr spin glass with a composition of $Fe_{17.8}Cr_{82.2}$ was studied in detail by means of NRSE. The microstructure was characterised by APT measurements, which show local concentration fluctuations of Fe and Cr on a length scale of 2 to 5 nm, which lead i) to the coexistence of ferro- and anti-ferromagnetic clusters and ii) a change of the magnetic properties of the whole sample, even in the spin glass phase, where spins are supposed to be randomly frozen. We show that a generalized spin glass relaxation function, which was successfully used to describe the phase transition in diluted spin glasses, can also be used for fitting the spin dynamics in spin glasses with significant concentration fluctuations.

Keywords: spin glasses; disordered systems; magnetism; neutron spin echo

---

1. Introduction

Spin glasses show frustrated magnetic interactions due to stochastically oriented spins and, thus, possess no magnetic long-range order. Typically, phase transitions in spin glasses occur at temperatures below 60 K. In spin glasses the disorder in the system at high temperatures, which is typically paramagnetic, reappears at low temperatures in a frozen state. Due to the frustration of the magnetic states in the spin glass phase, slow decay processes on large time scales may be observable [1]. Inelastic and quasi-elastic neutron scattering capture an important part of these slow relaxation processes [2,3]. On these data, models are based to describe the relaxation process in spin glasses. Pickup et al. suggested a generalized spin glass relaxation process [4] by connecting the probabilistic Weron model [5] and a model, which describes highly disordered systems on the basis of Lévy-stable distributions, firstly introduced by Tsallis [6]. Pickup used this model to describe successfully the relaxation processes in the diluted spin glass systems $Au_{1-x}Fe_x$ and $Cu_{1-x}Mn_x$ [4]. In this way it was shown that processes in spin glasses are similar to those in other complex disordered systems. In a few spin glass systems, the so called cluster spin glasses, clusters of magnetic order coexist with the magnetic amorphous spin glass phase [7]. However, only little is known about the relaxation processes in those cluster spin glasses.

In this contribution we study the relation between microstructure leading to magnetically ordered clusters and the averaged spin relaxation in a Fe-Cr sample, which shows a temperature driven phase transition to a cluster spin glass (SG) phase. For this purpose we combine two high resolution methods, namely the atomically resolved atom probe tomography (APT) [8–10] and the high resolution neutron

Preprints (www.preprints.org) | NOT PEER-REVIEWED | Posted: 27 June 2018 doi:10.20944/preprints201806.0435.v1

Peer-reviewed version available at Quantum Beam Sci. 2018, 2, 26; doi:10.3390/qubs2040026

(resonance) spin echo spectroscopy (N(R)SE). Additionally, magnetization measurements complete the characterization of the specimen.

APT measurements show that nanometer sized Cr rich regions coexist next to Fe rich regions. These may result in magnetically ordered clusters even in the spin glass phase. The shown results support the assumption, that the Weron model introduced by Pickup et al. [4] for diluted spin glasses like $Au_{1-x}Fe_x$ and $Cu_{1-x}Mn_x$ still works for spin glasses with inhomogeneities in the microstructure, if some of the parameters are restricted, however, the physical interpretation of the results may differ. The model will be explained in detail below. It is shown that even small scale inhomogenities in the microstructure may change the overall relaxation processes of spin glasses significantly. The relaxation process is then governed by different contributions of hierarchically ordered cluster interactions and parallel spin interactions compared to diluted spin glasses.

2. Experimental details

For this study a Fe-Cr alloy with a nominal composition of $c_{\mathrm{Fe}} = 14.5$ and $c_{\mathrm{Cr}} = 85.5$ at.% was used. The sample was prepared from starting materials with a purity of 99.99%, arc melted, annealed for 4 days at 1100°C and quenched in water. To relax the occurring strains, the sample was annealed at 1000°C for one day. The cylindrical sample has a height of approximately 20 mm and a diameter of about 10 mm. Atom probe tomography revealed an averaged chemical composition of $c_{\mathrm{Fe}} = 17.8$ and $c_{\mathrm{Cr}} = 82.2$ at.%. The concentration of impurities from the production process is approximately 0.01 at.% and thus neglectable. The phase diagram of the Fe-Cr-system is given by Burke et al. [11]. Based on the found chemical composition c_{Fe} and c_{Cr} the material is supposed to show no magnetic order and to transfer directly from the paramagnetic regime to the spin glass phase.

The ac susceptibility measurements were performed using a Quantum Design physical property measurement system (PPMS). An excitation amplitude of 1 mT with an excitation frequency between 10 Hz and 10 kHz was used.

The relaxation measurements were carried out on the neutron (resonance) spin echo spectrometers RESEDA [12] and JNSE [13] at the neutron source FRM II. The wavelength chosen was 5.5 Å for RESEDA and 5 Å for JNSE. At RESEDA, a range of spin echo times τ from approx. 0.05 ns to 1 ns was accessible. With JNSE the range could be extended to 10 ns. The τ-dependence of the polarization P of the neutrons was independent of the momentum transfer q. Thus, to improve measurement statistics, the experimental results are averaged for q values between $0.04\ \text{Å}^{-1} \leq q \leq 0.08\ \text{Å}^{-1}$. The intermediate scattering function $S(q, \tau)$ was determined for temperatures $T = 12.1$, 14.5, 19.4, 25.1, 30.1 and 34.2 K. After correcting the data for depolarization by the sample and the spectrometer at the different temperatures, the data sets are normalized to the intermediate scattering function as measured at $T = 3.6$ K, where the dynamics appears to be frozen on the time scales achieved by the spectrometers.

The atom probe tomography measurements were carried out with a Cameca LEAP 4000X HR system from Cameca located at the Karlsruhe Nano Micro Facility (KNMF). The atom probe tips were prepared by means of a focused ion beam with a Strata 400 system. The atom probe tips were measured in the voltage mode with a pulse rate of 200 kHz and a pulse fraction of 20% at a temperature of about 55.8 K. Analysis and reconstruction of the data was done with the IVAS 6.8.10 software package from Cameca.

3. Generalized spin glass relaxation model based on Weron

In the Weron model [5] the fractal character of the spin glass is described by the exponent β, whereas k is a measure for the contribution of hierarchical parallel and thus independent relaxation processes. Combined with the relaxation time τ, the generalized relaxation function based on the Weron model is given by

$$\varphi(t) = [1 + k(t/\tau)^{\beta}]^{-1/k}. \tag{1}$$

Preprints (www.preprints.org) | NOT PEER-REVIEWED | Posted: 27 June 2018 doi:10.20944/preprints201806.0435.v1

Peer-reviewed version available at Quantum Beam Sci. 2018, 2, 26; doi:10.3390/qubs2040026

In the Tsallis model [6] the sum of the entropy of two independent processes is larger or smaller than the direct sum of their entropies. The difference is scaled with the non-extensivity parameter q_T. Brouers and Sotolongo-Costa [14] showed, that there is a direct relation between the Tsallis and the Weron model when k is replaced by $k = (q_T - 1)/(2 - q_T)$. The application to spin glasses will be shortly described in the following and is explained in greater detail by Pickup et al [4]. Generally, the dynamics in a system slows down with decreasing temperature. This statement also applies for spin glasses. Thus, the lifetime of relaxation processes, τ, must increase with decreasing temperature. For the temperature limit $T \to 0$, $\tau \to \infty$ must apply.

Above the spin glass transition temperature, T_{SG}, spin-spin interactions are dominant. In the Weron model, this fact is expressed by a relatively large value of β ($\beta_{max} = 1$). Because the inter-cluster interactions are suppressed in the regime above T_{SG}, the value of k will be small. For high temperatures, where relaxation processes are dominated by thermal activation, $\beta = 1$ and $k \to 0$, i.e. the Weron model describes a pure exponential decay. For decreasing temperatures the spins are slowed down (until they are frozen) and the contribution of parallel, independent relaxation processes increases: The value of k increases, while β decreases. If all relaxation processes occur in single spin clusters, which do not interact with each other, k converges to infinity. In this limit $q_T = 2$ applies.

4. Results

The ac susceptibility measurements shown in figure 1 demonstrate that the sample exhibits a temperature driven spin glass (SG) phase transition near $T_{SG} \approx 25\,\mathrm{K}$. This value is consistent with results shown by Burke et al. for an iron concentration of $c_{Fe} \sim 17.8$ at.% [11]. As expected from the chemical composition there is no clear phase transition from the paramagnetic (PM) to a magnetically ordered phase for temperatures between 50 and 200 K in the ac susceptibility measurements.

Figure 2 a) shows the reconstructed APT with the elements Fe and Cr. The black box represents the area ($120 \times 30\,\mathrm{mm}^2$, length $\times$ height) in which the 2D concentration maps of Fe and Cr are shown after integration of the concentration along the depth (2.5 mm) of the sample. The resulting 2D concentration maps of Cr, Fe and Cr+Fe, as analyzed by the software IVAS are shown in figures 2 b-d). Impurities in the material, such as N and C from the production process and Ga from the FIB cut of the atom probe tip are locally far less than 0.05 at.%.

Figure 3 shows the intermediate scattering function versus the relaxation time as measured at RESEDA and JNSE together with fits to the Weron model given by equation 1. It is clearly seen that the spin fluctuations freeze with decreasing temperature T. For the fitting procedure the following two obvious assumptions were made: i) $0 \leq \beta \leq 1$. Of course, $\beta = 1$ above T_{SG} in the PM phase. Therefore, β can only decrease with decreasing T. ii) τ has to monotonically increase with decreasing T due to freezing. If the parameter k was not restricted, it increased with decreasing T, as one would expect because more and more independent relaxation processes can contribute to the dynamics. However, τ decreased which contradicts the physical intuition (dashed lines in Figure 4). Meaningful fits, i.e. a decreasing τ was only obtained if k was constrained to a constant value for all $T \leq T_{SG}$. The exact value was hard to determine and was found to be $k \leq 4$. All values $k \leq 4$ led to a physically meaningful decrease of τ with decreasing temperature.

Of course, the exact values of the fit parameters depend strongly on the chosen value of k, thus exact values of the fit parameters cannot be extracted. The following discussion is based on fit results obtained with a constant $k = 2.5$. Figure 4 shows the resulting temperature dependence for k, β and τ with the restriction of $k = 2.5$ (solid lines and closed symbols) compared to fit results with no boundary conditions except $0 \leq \beta \leq 1$ (dashed lines with open symbols). Table 1 shows all values of the intermediate scattering function in dependence of the spin echo times for all temperatures, so that the fit values might be reproduced by interested readers.

Preprints (www.preprints.org) | NOT PEER-REVIEWED | Posted: 27 June 2018 doi:10.20944/preprints201806.0435.v1
Peer-reviewed version available at Quantum Beam Sci. 2018, 2, 26; doi:10.3390/qubs2040026

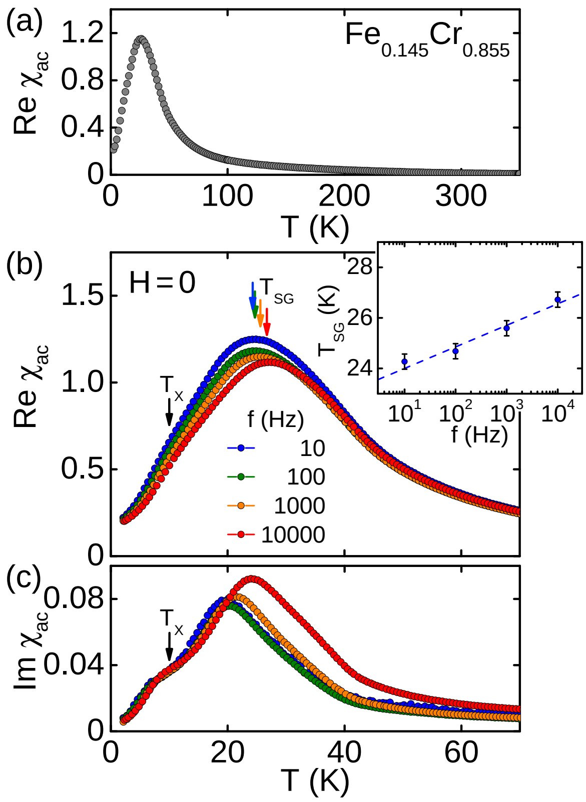

Figure 1. Temperature dependence of the ac susceptibility of the studied sample. (a) Real part of the ac susceptibility between 2 K and 350 K measured at 911 Hz. The absolute value is large, when compared with a typical antiferromagnetic compound. (b) Real part of the ac susceptibility, Re χ_{ac}, as measured at low temperatures for excitation frequencies between 10 Hz and 10 kHz. As depicted in the inset and characteristic for a spin glass, the position of the maximum at T_{SG} shifts clearly as a function of the excitation frequency. (c) Imaginary part of the ac susceptibility, Im χ_{ac}, at low temperatures. A change of slope at $T_x \sim 10$ K in Re χ_{ac} and, in particular, in Im χ_{ac} suggests the presence of an additional transition, which is not captured in the neutron data and will not be considered further.

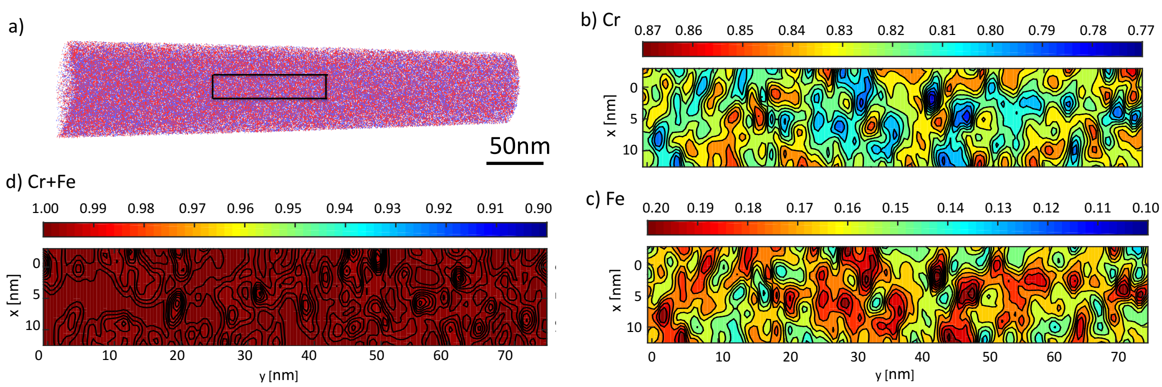

Figure 2. a) Atom probe reconstruction of the Fe-Cr alloy, measured at 50 K. The black box marks the area were the data for the 2D concentration maps b) and c) are taken from. Clearly visible are small clusters of Cr and Fe, respectively. The concentration distribution is integrated over a sample slice with a thickness of 2.5 nm. d) shows the summation of b) and c), which should sum up to 100%. The small differences of less than 1% are caused by impurities such as P, N, and Ga.

Preprints (www.preprints.org) | NOT PEER-REVIEWED | Posted: 27 June 2018 doi:10.20944/preprints201806.0435.v1

Peer-reviewed version available at Quantum Beam Sci. 2018, 2, 26; doi:10.3390/qubs2040026

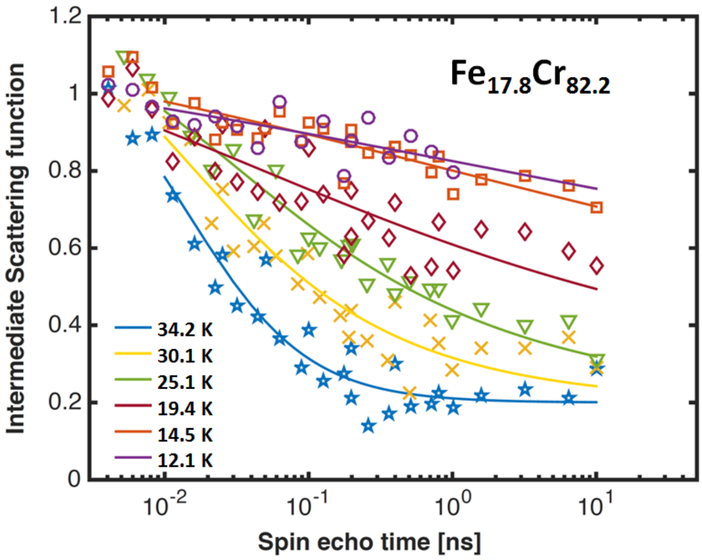

Figure 3. Intermediate scattering function as measured by neutron (resonance) spin echo at RESEDA and at JNSE for $q \simeq 0.06$ Å^{-1}. The solid lines show the restricted Weron model fitted to the experimental data (symbols) assuming $k = 2.5$ for $T \leq T_{SG}$. The parameters of the fit are shown in figure 4.

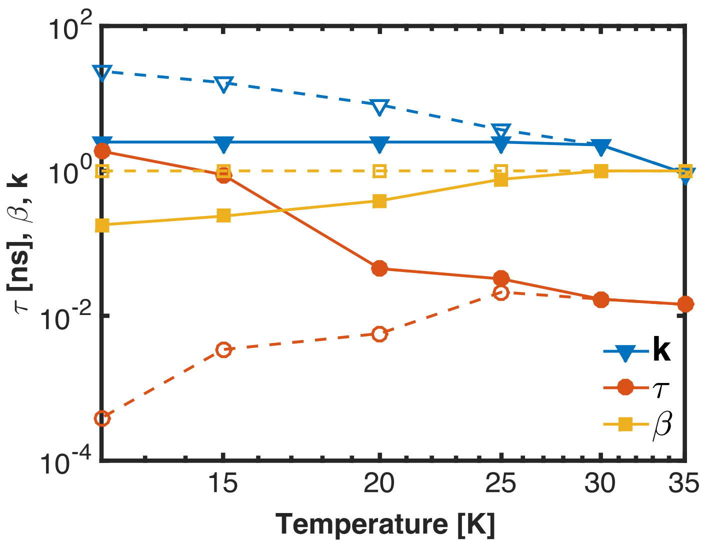

Figure 4. Parameters τ, β and k analysed by a fit of the Weron function to the intermediate scattering functions observed for different temperatures by N(R)SE measurements with no restrictions except $0 \leq \beta \leq 1$ (dashed lines and open symbols) and with restrictions i) $0 \leq \beta \leq 1$, ii) τ constantly increasing with decreasing T and iii) $k = 2.5$ for $T \leq 25$ K (solid lines and closed symbols).

Peer-reviewed version available at Quantum Beam Sci. 2018, 2, 26; doi:10.3390/qubs2040026

5. Discussion

The spin glass transition temperatures $T_{\rm SG} \sim 25\,K$ as measured by means of ac susceptibility and neutron scattering are consistent with each other. For N(R)SE, the transition might be identified due to the observation that the time dependence becomes more exponential with increasing temperature. $T_{SG} \sim 25\,K$ is also consistent with the value given by Burke et al. [11] for an iron concentration of $c_{\rm Fe} = 17.8$ at.%. The susceptibility measurements show that there is no other phase transition for $T > T_{\rm SG}$, indicating that there is no magnetically ordered phase in the material (figure 1). A change of slope at $T_x \sim 10$ K in Re $\chi_{\rm ac}$ and in particular in Im $\chi_{\rm ac}$ suggests the presence of an additional transition, which shows no signature in the neutron scattering data and will not be considered further.

The atom probe tomography studies clearly show, that Fe rich regions coexist with Cr rich regions in the material (figure 2). In those zones, the concentration of Fe might be high or low enough, that ferromagnetic (FM) or antiferromagnetic (AFM) ordering will be observed. According to Burke et al. [11] an Fe concentration of about 19 at% for FM ordering and of 16 at% for AFM ordering is necessary for temperatures lower than ~ 50 K. Figure 2 shows that those values are reached locally over a length scale of approximately 2–5 nm.

According to Burke et al. [11] and Fincher and Shapiro et al. [15,16], the Néel temperature for concentrations of $c_{\rm Fe}$ of 14 at.% is supposed to be $T_N \sim 60$ K. The Curie temperature for $c_{\rm Fe} = 20$ at.% is $T_C \sim 80$ K. Thus, with decreasing T a change in polarization and intensity of the neutron signal around $q = 0.06$ Å^{-1} is expected as follows: Approaching T_C from high temperatures will initiate the formation of ferromagnetic clusters, which reduces the polarization of the scattered neutrons. Decreasing T further towards T_N leads to the formation of antiferromagnetic ordering in regions surrounding the ferromagnetically ordered regions. Thus the size of the ferromagnetic clusters decreases, resulting in an increase in polarization. Lowering T further favors the spin glass phase thus shrinking the regions of both, ferromagnetic and antiferromagnetic phase further thus leading to a continuing increase of intensity and polarization with decreasing T.
Indeed these trends can be qualitatively observed in the neutron scattering data. Figure 5 shows the neutron polarization and the intensity of the neutrons at $q = 0.06$ Å^{-1} with decreasing T. The polarization decreases with decreasing T, reaches a minimum around 120 K and increases again. The deviation from the expected minimum around 80 K may be due to the volume averaging and q-weighting by the neutrons. Overall, an increase in neutron intensity is observed as expected.

To put our results on a more quantitative basis we estimate the size of the ferromagnetic clusters using the expression for the polarization of the neutrons $P = P_0 \exp(-\frac{1}{3}\gamma^2\langle B^2\rangle \frac{\delta}{v^2} d_{\rm eff})$ derived by Halpern and Holstein [17] in the limit of small fields and domains. P is a function of the gyromagnetic ratio $\gamma = 2.916$ kHz/Gauss, the magnetic field B, the domain size of the ferromagnetic clusters δ, the effective sample thickness for iron $d_{\rm eff}$, and the velocity of the neutrons v. The velocity of neutrons with a wavelength of $\lambda = 5.5$ Å is $v \approx 720$ m/s. For the magnetization of the Fe clusters we assumed the bulk magnetization of Fe $\mu_{\rm M} = 1.74$ T [**?**]. With $d_{\rm eff} = d_{\rm bulk} c_{\rm Fe} = 10\,{\rm mm} \cdot 0.145 \sim 1.38$ mm an approximate cluster size of ~ 200 Å for temperatures between 250 and 120 K is obtained. For the final polarization measured in our experiment (about 28%) at 8 K this assumption corresponds to a size of the ferromagnetic clusters of $\delta \sim 140$ Å. This is still considerably larger than the regions of high Fe concentrations in the APT analysis, which scale to 2 – 5 nm. However, the conclusion, what can be drawn from APT and N(R)SE is similar: In regions of high Fe concentration the ferromagnetic order might still be present, even if those regions are surrounded by pure spin glass phase. The same holds true for the regions of high Cr concentration, where the antiferromagnetic ordering might still be present. Both phenomena lead to islands of magnetic ordering in the spin glass phase.

Based on the above discussion the results of the N(R)SE experiments can be interpreted as follows: For $T > T_{\rm SG}$ the sample is magnetically ordered in locally restricted areas as indicated by the ATP-data, leading to a maximum value $\beta = 1$ and a minimal value of k, as seen in figure 4. Regions of magnetic fluctuations are present but their parallel hierarchical relaxation processes have only a small weight when compared to the spin-fluctuations within the ordered clusters. With decreasing T, the volume

Preprints (www.preprints.org) | NOT PEER-REVIEWED | Posted: 27 June 2018 doi:10.20944/preprints201806.0435.v1

Peer-reviewed version available at Quantum Beam Sci. 2018, 2, 26; doi:10.3390/qubs2040026

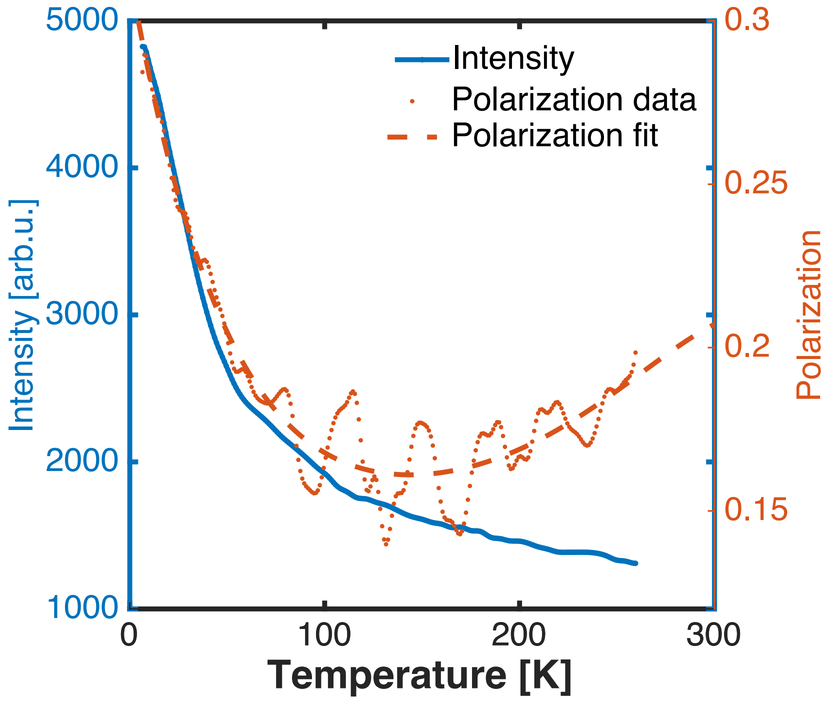

Figure 5. Temperature dependence of the intensity (blue) and the polarization (orange) as measured at $q = 0.06$ Å^{-1} at RESEDA. The data are recorded during the course of cooling down the sample. Data recorded during heating up the sample give similar results (not shown), thus hysteresis effects do not play a role.

fraction of the sample, where the spin fluctuations slow down increases and thus the contribution of the parallel relaxation processes increases due to the decreasing size of magnetically ordered clusters. The value of k increases, while β decreases. In diluted spin glasses k is supposed to diverge to infinity ($q_T \to 2$), because relaxation processes on all time scales occur. In our sample, however, the value of k converges to a constant value (figure 4). The value of k is constrained because of the limited number of parallel processes due to the remaining clusters, which are directly observed by ATP and indicated by the finite polarization of the neutrons at low T.

Figure 6 shows a comparison of the results obtained from the diluted spin glass systems $Au_{1-x}Fe_x$ and $Cu_{1-x}Mn_x$ as studied by Pickup [4] and the results of our work. The major difference between the two data sets below T_{SG} reflects the different mechanisms taking place during the spin freezing. Whereas in diluted spin glasses all spins are frozen in random orientations, in the Fe-Cr system ferromagnetic and antiferromagnetic clusters coexist within a sea of disordered spin glass phase. Therefore, the hierarchical order of relaxation processes changes from only parallel relaxation processes to spin-spin and parallel relaxation processes. Since our study already showed the complementation of scattering methods and atom probe tomography, the further investigations must concentrate on the study of the short range order of Fe-Cr alloys in dependence of the found clusters. Here, special emphasis will be laid on the influence of the heat treatment of the material on both the phase transition and the short range order in the spin glass phase, because Fe-Cr alloys are known for their clustering and spinodal decomposition [18]. Also the phase transition at $T \sim 10\,\mathrm{K}$ needs further attention to be fully identified.

6. Conclusions

By combining atomically resolved atomic probe tomography (APT) with quasielastic neutron scattering using N(R)SE we have characterized the evolution of the spin glass phase in the presence

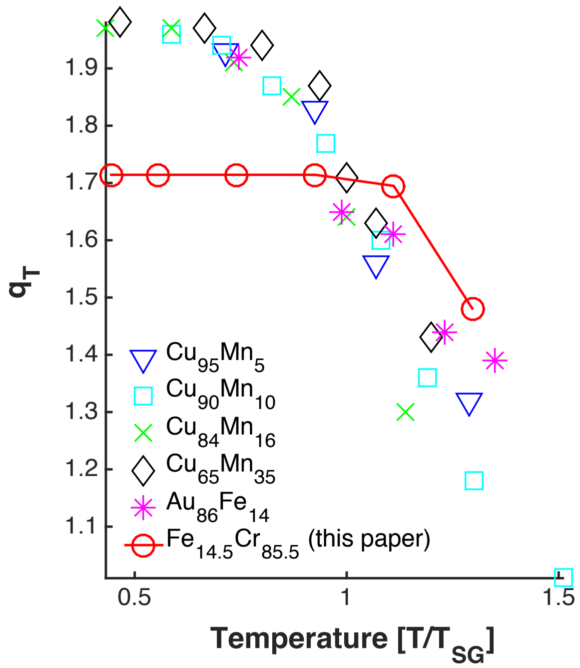

Figure 6. Comparison between data published by Pickup [4] on diluted spin glasses $Au_{1-x}Fe_x$ and $Cu_{1-x}Mn_x$ and the results observed in the present study on the cluster spin glass $Fe_{17.8}Cr_{82.2}$.

of ferro- and antiferromagnetic clusters in the cluster spin glass $Fe_{17.8}Cr_{82.2}$. The measured data can be interpreted in terms of the Weron model that assumes the decay of spin fluctuations in parallel processes in the presence of magnetically ordered clusters. Our results may also be relevant to other cluster-type spin glasses.

Acknowledgments: We thank the FRM II for providing beam time at the neutron resonance spin echo spectrometer RESEDA and the JCNS for providing beam time at the spectrometer JNSE. The work at Brookhaven was supported by the Office of Basic Energy Sciences, Division of Materials Science and Engineering, U.S. Department of Energy (DOE) under Contract No. DEAC02-98CH10886.

Author Contributions: J. N. W. leading scientist for experiments (neutrons and APT), analysis and interpretation of the data; W. H. and O. H. instrument responsible of RESEDA and NRSE, respectively, supported before, during and after the neutron experiments, discussed analysis and interpretation of the data; A. B. conducted the ac susceptibility measurements and interpreted them; S. M. S. provided the sample material; P. B. supported all steps of the experiment, the interpretation of the data and improved the paper. All authors reviewed the manuscript.

Conflicts of Interest: The authors declare no conflicts of interest. The founding sponsors had no role in the design of the study; in the collection, analyses, or interpretation of data; in the writing of the manuscript, and in the decision to publish the results.

Abbreviations

The following abbreviations are used in this manuscript:

APT	atom probe tomography
FWHM	full width at half maximum
ISF	intermediate scattering function
KNMF	Karlsruhe Nano Micro Facility
N(R)SE	neutron (resonance) spin echo
NSE	neutron spin echo
PM	paramagnetic
PPMS	physical property measurement system
RF	radio frequency
SET	spin echo time
SG	spin glass

References

1. A. P. Ramirez, Strongly geometrically frustrated magnets. *Annu. Rev. Mater. Sci.* **1994**, *24*, 453-480.
2. W. Bao, S. Raymond, S. M. Shapiro, K. Motoya, B. Fåk and R.W. Erwin, Unconventional Ferromagnetic and Spin-Glass States of the Reentrant Spin Glass $Fe_{0.7}Al_{0.3}$. *Phys. Rev. Let.* **1999**, 82, 4711-4714.
3. A. P. Murani and J. L. Tholence, Spin Dynamics of a Binary Alloy (Spin Glass). *Solid State Commun.* **1977**, 22, 25-28.
4. R. M. Pickup, R. Cywinski, C. Pappas, B. Farago and P. Fouquet, Generalized Spin-Glass Relaxation. *Phys. Rev. Lett.* **2009**, 102, 097202.
5. K. Weron, How to obtain the universal response law in the Jonscher screened hopping model for dielectric relaxation. *J. Phys. Condens. Matter* **1991**, 3, 231-233.
6. C. Tsallis, S. V. F. Levy, A. M. C. Souza and R. Maynard, Statistical-Mechanical Foundation of the Ubiquity of Lévy Distributions in Nature. *Phys. Rev. Lett.* **1995**, 75, 3589-3593.
7. M. Gabay and G. Toulouse, Coexistence of Spin-Glass and Ferromagnetic Orderings. *Phys. Rev. Lett.* **1981**, 47, 201-204.
8. B. Gault, M. P. Moody, J. M. Cairney, and S. P. Ringer, *Atom Probe Microscopy*, Springer Science & Business Media, New York, NY, 2012; ISBN 978-1-4614-3436-8.
9. D. J. Larson, T. J. Prosa, R. M. Ulfig, B. P. Geiser, and Th. F. Kelly, *Local Electrode Atom Probe Tomography*, Springer: New York, NY, 2013; ISBN 978-1-4614-8721-0.
10. M. K. Miller, *Atom Probe Tomography*, Springer: Boston, MA, 2014; ISBN 978-1-4615-4281-0.
11. S. K. Burke, R. Cywinski, J. R. Davis and B. D. Rainford, The evolution of magnetic order in CrFe alloys. II. Onset of ferromagnetism. *J. Phys. F* **1983**, 13, 451-470.
12. W. Häussler, P. Böni, M. Klein, C. J. Schmidt, U. Schmidt, F. Groitl and J. Kindervater, Detection of high frequency intensity oscillations at RESEDA using the CASCADE detector. *Rev. Sci. Instrum.* **2011**, 82, 045101.
13. O. Holderer, M. Monkenbusch, R. Schätzler, H. Kleines, W. Westerhausen and D. Richter, The JCNS neutron spin-echo spectrometer J-NSE at the FRM II. *Meas. Sci. Technol.* **2008**, 19, 034022.
14. F. Brouers and O. Sotolongo-Costa, Universal relaxation in nonextensive systems. *Europhys. Lett.* **2003**, 62, 808-814.
15. C. R. Fincher, Jr., S. M. Shapiro, A. H. Palumbo, R. D. Parks, Spin-Wave Evolution Crossing From the Ferromagnetic to Spin-Glass Regime of Fe_xCr_{1-x}, *Phys. Rev. Lett.* **1980**, 45, 474-477.
16. S. M. Shapiro, C. R. Fincher, Jr., A. C. Palumbo, and R. D. Parks, Anomalous spin-wave behavior in the magnetic alloy Fe_xCr_{1-x}. *Phys. Rev. B* **1981**, 24, 6661-6674.
17. O. Halpern and T. Holstein, On the Passage of Neutrons Through Ferromagnets. *Phys. Rev.* **1941**, 59, 960-981.
18. M. K. Miller, J. M. Hyde, M. G. Hetherington, A. Cerezo, G. D. W. Smith, and C. M. Elliott, Spinodal Decomposition in Fe-Cr Alloys: Experimental Study at the Atomic Level and Comparison with computer Models - I. Introduction and Methology. *Acta Metall. Mater.* **1995**, 43, 3385-3401.

Table 1. Spin echo time (SET) and values of the intermediate scattering function (ISF) for all measured temperatures ($12.1 \leq T \leq 34.2\,\mathrm{K}$).

SET [ns]	ISF 12.1K	error 12.1K	SET [ns]	ISF 14.5K	error 14.5K	SET [ns]	ISF 19.4K	error 19.4K
0.00409	1.02276	0.06006	0.00409	1.05768	0.05938	0.00409	0.98686	0.05903
0.00602	1.00878	0.05935	0.00602	1.09378	0.06067	0.00602	1.06622	0.06179
0.00813	0.96591	0.05791	0.00813	1.01485	0.05781	0.00813	0.95992	0.05795
0.01145	0.92834	0.0538	0.01145	0.92272	0.05197	0.01145	0.82503	0.05063
0.01617	0.91736	0.05504	0.01617	0.97386	0.05513	0.01617	0.88892	0.05423
0.02253	0.93979	0.05484	0.02253	0.88035	0.05109	0.02253	0.79933	0.05037
0.03181	0.91483	0.05615	0.03181	0.90611	0.05406	0.03181	0.77239	0.05158
0.04465	0.85836	0.05449	0.04465	0.88378	0.0536	0.04465	0.74521	0.05102
0.06279	0.97755	0.06212	0.06279	0.95468	0.05939	0.06279	0.71707	0.05341
0.08888	0.87447	0.05982	0.08888	0.87917	0.0582	0.08888	0.72044	0.05503
0.12548	0.92691	0.06301	0.12548	0.90804	0.06025	0.12548	0.7405	0.05691
0.17724	0.78653	0.05843	0.17724	0.76687	0.05573	0.17724	0.5812	0.05268
0.19732	0.87647	0.06422	0.19732	0.90613	0.0629	0.19732	0.63119	0.05613
0.26199	0.93792	0.06647	0.26199	0.84559	0.06081	0.26199	0.66925	0.05729
0.36492	0.8335	0.0552	0.36492	0.84718	0.05369	0.36492	0.62548	0.04892
0.51595	0.89125	0.05869	0.51595	0.8401	0.05497	0.51595	0.52864	0.048
0.71752	0.85023	0.07396	0.71752	0.79749	0.06927	0.71752	0.55169	0.06368
1.01391	0.79711	0.07074	1.01391	0.73849	0.06605	1.01391	0.54046	0.06272
			0.02529	0.92578	0.0217	0.02543	0.91805	0.02341
			0.04978	0.90893	0.02173	0.04989	0.90867	0.02357
			0.0998	0.92581	0.02124	0.1003	0.8605	0.02246
			0.19972	0.8752	0.01941	0.19945	0.74776	0.0202
			0.39854	0.86228	0.01845	0.39976	0.71885	0.0191
			0.79839	0.83665	0.01753	0.79888	0.66614	0.01803
			1.59816	0.7778	0.01495	1.59894	0.64925	0.01571
			3.19855	0.7861	0.01559	3.19747	0.64314	0.0161
			6.39774	0.76103	0.01594	6.39856	0.59164	0.01658
			9.9985	0.70518	0.02048	9.99848	0.55466	0.0217
SET [ns]	ISF 25.1K	error 25.1K	SET [ns]	ISF 30.1K	error 30.1K	SET [ns]	ISF 34.2K	error 34.2K
0.00526	1.09754	0.06667	0.00525	0.96771	0.0617	0.00409	1.01164	0.06198
0.00754	1.03817	0.06788	0.00765	1.00928	0.06715	0.00602	0.88442	0.05747
0.01079	0.99185	0.06757	0.01082	0.92648	0.06523	0.00813	0.89517	0.05781
0.01512	0.88966	0.06278	0.01508	0.88101	0.06266	0.01145	0.73806	0.04983
0.02125	0.80296	0.05852	0.02125	0.66394	0.05382	0.01617	0.61188	0.04774
0.03002	0.85592	0.06467	0.02987	0.59078	0.05516	0.02253	0.49692	0.04387
0.04216	0.67408	0.05884	0.04217	0.60437	0.0567	0.03181	0.44948	0.04482
0.05965	0.8016	0.06767	0.05955	0.57911	0.05997	0.04465	0.42374	0.04469
0.08404	0.58313	0.06082	0.08394	0.50844	0.05899	0.06279	0.36484	0.04685
0.11873	0.60005	0.06782	0.11872	0.4726	0.06416	0.08888	0.28966	0.04716
0.16803	0.57163	0.08267	0.16771	0.42479	0.0778	0.12548	0.25518	0.04778
0.19188	0.60791	0.09113	0.19179	0.37019	0.0829	0.17724	0.27402	0.04849
0.25498	0.50625	0.07413	0.25486	0.36084	0.07005	0.19732	0.21112	0.05007
0.355	0.56178	0.06561	0.35483	0.30882	0.059	0.26199	0.14018	0.04911
0.50215	0.51515	0.07345	0.50191	0.22345	0.06644	0.36492	0.1709	0.04189
0.70143	0.49382	0.10095	0.70109	0.41314	0.09901	0.51595	0.19155	0.04417
0.9911	0.41238	0.09801	0.99062	0.28469	0.09488	0.71752	0.19639	0.05956
0.09993	0.62805	0.02397	0.02534	0.75225	0.02896	1.01391	0.18747	0.05861
0.20028	0.61087	0.02242	0.04913	0.66412	0.02883	0.02533	0.58292	0.03211
0.39978	0.48247	0.02087	0.09842	0.58733	0.02762	0.05043	0.56945	0.03201
0.79925	0.49432	0.02003	0.19907	0.43724	0.02542	0.09976	0.38865	0.03089
1.59864	0.44597	0.01732	0.40046	0.45993	0.02417	0.19893	0.34034	0.02876
3.19816	0.40069	0.01767	0.79944	0.3529	0.02284	0.39957	0.29977	0.02729
6.3974	0.41392	0.01823	1.59859	0.34077	0.01993	0.79908	0.2258	0.02593
9.99879	0.31263	0.02397	3.19825	0.34015	0.02046	1.59863	0.21929	0.02263
			6.39851	0.36829	0.02118	3.19827	0.23321	0.0233
			9.99884	0.29178	0.02805	6.3991	0.21245	0.02436
						9.99846	0.28799	0.03217